Instruments and Methods

An automated submersible flow cytometer for analyzing pico- and nanophytoplankton: FlowCytobot

Robert J. Olson*, Alexi Shalapyonok, Heidi M. Sosik

Woods Hole Oceanographic Institution, Woods Hole, MA 02543, USA

Abstract

Flow cytometry is a valuable tool for the analysis of phytoplankton and other suspended particles because of its speed and quantitative measurements, but the method's oceanographic application has been limited by the need to take discrete water samples for analysis on board ship or in the laboratory. For this reason, we have developed an automated flow cytometer (FlowCytobot) that can operate in situ and unattended. The new instrument utilizes a diode-pumped 532 nm laser and can measure light scattering and fluorescence of particles as small as *Synechococcus* cells. For operation at the LEO-15 mooring site off New Jersey, it is connected to shore by power and communications cables, and is controlled by a microcomputer whose programming can be loaded remotely. The sampling rate is adjustable; we have used from 12.5 to 50 μl min^{-1}. Integrated signals from each particle (two light scattering angles and two fluorescence emission bands) are transmitted to a shore-based computer, where they are accessible by Internet and can be examined in real time. FlowCytobot was deployed at LEO-15 from late July to early October 2001, where it operated continuously (aside from occasional power or communications interruptions at the node) without outside intervention. Even after 2 months of in situ operation, FlowCytobot's measurements were similar to those of a conventional flow cytometer, as shown by analysis of a discrete water sample taken at the location of the sample inlet. In addition to documenting seasonal and event-scale changes in size distributions and population abundances in the pico- and nanophytoplankton, FlowCytobot will be useful for examining diel cycles in light scattering and pigment fluorescence of cells in situ that may allow estimation of rates of production by different phytoplankton groups.
© 2003 Elsevier Science Ltd. All rights reserved.

Keywords: Phytoplankton; Flow cytometry; Mooring; Time series; Fluorescence; Scattering

1. Introduction

Detailed knowledge of the composition and characteristics of the particles suspended in the sea is crucial to an understanding of the biology, optics and geochemistry of the oceans. The composition and size distribution of the phytoplankton community, for example, help determine the flow of carbon and nutrients through an ecosystem (Chisholm, 1992), and can be important indicators of change in coastal environments subject to anthropogenic disturbances such as nutrient loading and pollution (Cloern, 2001). Flow cytometry, which provides rapid and quantitative measurements of individual suspended microscopic particles, has proved a

*Corresponding author. Tel.: +1-508-289-2565; fax: +1-508-457-2169.

E-mail address: rolson@whoi.edu (R.J. Olson).

valuable tool for studies of cells in the size range ∼ 0.5–30 μm (Olson et al., 1991, 1993; Vaulot et al., 1995; Vaulot and Marie, 1999; Reckermann and Colijn, 2000; Li and Dickie, 2001). In a flow cytometer, several optical measurements are made as each particle in a water sample passes through a focused laser beam. Light scattering signals provide information about the distributions of particle size and composition, while fluorescence data allow discrimination between phytoplankton and other particles, and identification of major phytoplankton groups. Time series of flow cytometric measurements have contributed to our understanding of phytoplankton species succession (Olson et al., 1990a; DuRand et al., 2001; Li and Dickie, 2001) and growth processes (DuRand and Olson, 1998; Shalapyonok et al., 1998; André et al., 1999; Jacquet et al., 2001; Shalapyonok et al., 2001) and of the effects of phytoplankton growth on bulk water optical properties (DuRand and Olson, 1996).

Although flow cytometry has provided new insights about pico- and nanoplankton, its use has been limited by the need to take discrete water samples for analysis on board ship or in the laboratory. This means that the sampling resolution, frequency and duration of studies are limited by the availability of ship time and wire time. Continuous, extended time series studies will allow us to investigate the responses of an ecosystem to environmental changes on several scales, including the diel cycle of light and dark, events such as storms and upwelling, and seasonal progressions. For these reasons, we have developed a submersible flow cytometer, FlowCytobot, which can operate in situ and unattended.

FlowCytobot's design is similar to that of laboratory-based flow cytometers in that a seawater sample is injected into the center of a sheath flow of particle-free water, which serves to confine all the particles to the center of the flow cell (and thus to uniform illumination by a focused laser beam). Because we originally assumed that such a flow system would be too easily contaminated or disturbed to work in the marine environment for extended periods, our first design incorporated a simple ducted flow of raw seawater in which the analysis region was optically defined by intersecting orthogonal laser beams: only particles which passed through both beams simultaneously were analyzed. We found that such an approach was workable, but the complexities and compromises it entailed persuaded us to return to the "conventional" fluid focusing approach. FlowCytobot differs from laboratory flow cytometers in that it is contained in a watertight pressure housing, but more significantly, it operates continuously and autonomously, under the direction of a microcomputer whose programming can be modified by a remote operator. Programmable operations include data acquisition and transfer to shore, adjustment of sampling frequency and rate of injection, injection of internal standard beads, flushing the flow cell or sample tubing with detergent, backflushing the sample tubing to remove potential clogs, adding sodium azide to the sheath reservoir to prevent biofouling of the internal surfaces, and adjustment of the laser steering mirror.

FlowCytobot is similar to another autonomous instrument, CytoBuoy (Dubelaar et al., 1999), in that it recycles sheath fluid and uses a diode-pumped laser, but it differs in important ways. FlowCytobot is linked to shore by power and communications cables, while CytoBuoy is battery powered and transmits data to shore by radio. These features allow CytoBuoy more flexibility as to location, but limit its duty cycle and data transmission rate. The number of ocean observatories suitable for deployment of instruments like FlowCytobot is small at present (we are aware of 3), but we anticipate a growing network of such sites, in open ocean as well as coastal waters (Glenn et al., 2000b).

The LEO-15 observatory includes two permanent underwater nodes with ports for providing in situ instruments with power and data connections to a shore lab. A variety of continuous measurements are available at the nodes (although for most of our deployment only bottom temperature and wave height were being measured), and meteorological and other environmental measurements are available from the shore station (Glenn et al., 2000a). The observatory is an ideal location to study effects of environmental forcing on plankton community structure. Southwesterly

winds along the coast cause recurrent upwelling to occur at LEO-15 during the summertime, with consequent nutrient enrichment and phytoplankton blooms. Suspended particles (from both phytoplankton growth and resuspension of sediment) can increase in concentration during these upwelling episodes (Schofield et al., 2002); upon cessation of upwelling (due to changing winds), water column stratification and remineralization processes can deplete dissolved oxygen (Pearce et al., 1982), damaging benthic organisms and fisheries. Storms may also interrupt these processes by re-mixing the water column. During the evolution of a bloom, species succession has been observed, with a diatom-dominated crop during upwelling giving way to dinoflagellates upon stratification (Kerkhof et al., 1999); presumably these kinds of changes in community composition will be reflected in cell size distributions as well.

2. Methods and materials

2.1. Instrument overview

FlowCytobot is based on a 532 nm solid-state laser for excitation, combined with a quartz flow cell and photomultiplier detectors for light scatter-

ing and fluorescence. A sampling valve system selects from ambient seawater, and reservoirs of solutions containing detergent or standard microspheres for calibration. Sheath water is recirculated during operation. The self-contained underwater system includes signal processing electronics and a computer for sample control and data acquisition. Power supply to the instrument, real-time data transmission to a shore-based computer, and user-initiated communication to change instrument status were accomplished via the cables to the permanent underwater node at the sampling site.

2.1.1. Fluidics

Seawater is drawn to the instrument housing (Fig. 1) through a 2 mm copper screen (to eliminate large particles) by a SeaBird pump on the outflow side ($\sim 1\,l\,min^{-1}$). Inside the housing, a programmable syringe pump with a 6-way distribution valve (Kloehn, Inc.) samples this flow through an 80 µm Nitex mesh on the end of 0.5 mm ID PEEK tubing. The sample is pumped and injected into the center of a sheath of particle-free (0.2 µm-filtered) seawater flowing at a rate of 5 ml min^{-1} through a flow cell with dimensions 180 µm $\times$ 400 µm. The rate of sample injection is adjusted so that the particles in the sample pass
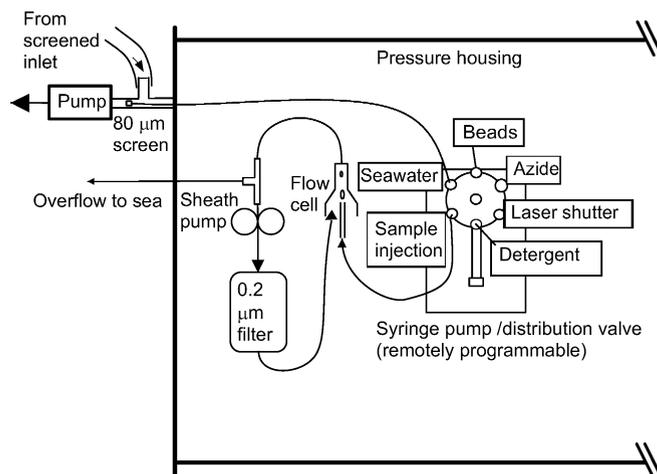
Fig. 1. Schema of fluidics system. The distribution valve at the syringe pump allows access to several reservoirs inside the instrument. Beads are injected periodically to monitor performance, sodium azide is added to the sheath fluid to prevent internal fouling, and detergent can be added to the flow cell and tubing (during this operation, the sheath pump is stopped and the laser is blocked by a hydraulically operated shutter).

one at a time through a laser beam; at present we inject sample seawater with a 0.25-ml syringe at 12.5–50 μl min^{-1}. Sheath fluid (seawater) is recirculated through a 0.2 μm cartridge filter by a miniature gear pump (MicroPump model 188 with PEEK gears and 1.6 mm ID PEEK tubing); the excess volume due to injection of sample overflows to the outside of the housing.

2.1.2. Optics and signal processing

The laser (532-nm, 100 mW diode-pumped solid state laser, Coherent, Inc.) beam, which is diverging in the horizontal direction, is focused by a spherical lens (20-mm focal length) to provide an elliptical beam spot with vertical and horizontal dimensions of 5 μm $\times$ 100 μm (Fig. 2). As each particle passes through the beam, it scatters laser light in the forward and side directions, and may emit red fluorescence from chlorophyll and orange fluorescence from phycoerythrin. This light is collected by lenses and directed by dichroic filters and mirrors to four independent photomultiplier tubes (PMTs) with appropriate optical filters, and converted to voltage signals by preamplifiers whose design follows that of the Coulter EPICS flow cytometer (R. Auer, pers. comm.). Signals are

Fig. 2. Schema of optical system showing light path of the excitation laser beam and collection of scattered (forward and side angles) and fluoresced light of the wavelengths indicated, in relation to the flow cell. Water samples containing particles are injected into the central channel of the flow cell as described in Fig. 1.

integrated during the time that they are above an adjustable threshold level. The logic circuitry can be configured to allow any of the signals to trigger digitization and storage of the integrated signals from all four detectors; at present we use chlorophyll fluorescence to trigger acquisition.

The instrument was constructed on an optical bench (12 in $\times$ 24 in) using off-the-shelf components, except for the signal processing and power supply boards, which were custom designed (Fig. 3). The flow cell (modified for pressures up to 130 psi by machining o-ring grooves for larger o-rings between the flow cell and its housing) and the fluorescence collection lens were from a FACScan flow cytometer (BD Biosystems). The forward light scattering lens was from a Coulter EPICS flow cytometer. Optical mounts were obtained from Newport Corp. and Thor Labs, Inc.; optical filters (532DF10 for scattered laser light, 680DF40 for chlorophyll, and 574DF40 for phycoerythrin fluorescence) and dichroics (630 nm short pass, 550 nm long pass) were from Omega Optical and Andover Optical. To detect green and orange light we used miniature modular PMTs from Hamamatsu (HC140-A); for chlorophyll fluorescence, which requires high red sensitivity, we used a Hamamatsu R1477 side-on tube (with HC123-01 integrated socket-HV supply). The PMT signals were linearly amplified; to increase the dynamic range of the measurements, a pair of amplifiers, with 30-fold difference in gains, was used for each signal. After integrating the signals to 14-bit precision and choosing the appropriate signal from each pair, we obtain about 4 decades of useful dynamic range. This allows us to measure signals from *Synechococcus* ($\sim$1 μm) up to $\sim$10 μm phytoplankton cells.

2.1.3. Control system

All functions of the instrument are controlled by an on-board microcomputer (Tattletale 8, Onset Computer Corp.), according to a program loaded from a shore-based computer. The shore computer can be operated locally or by remote control over the Internet (using PCAnywhere software and a modem-controlled power switch). The data are displayed in real time as 2-parameter dot plots for monitoring performance. Because we found that
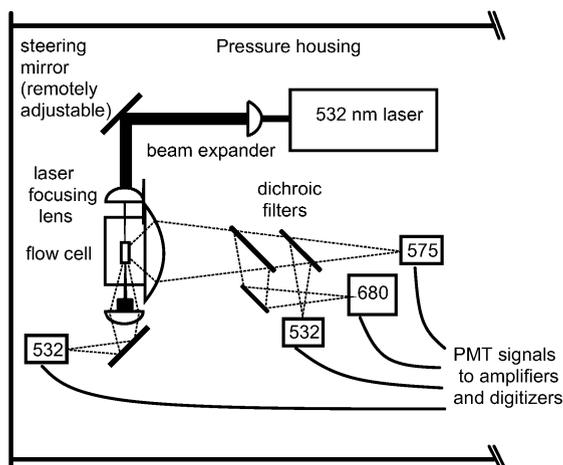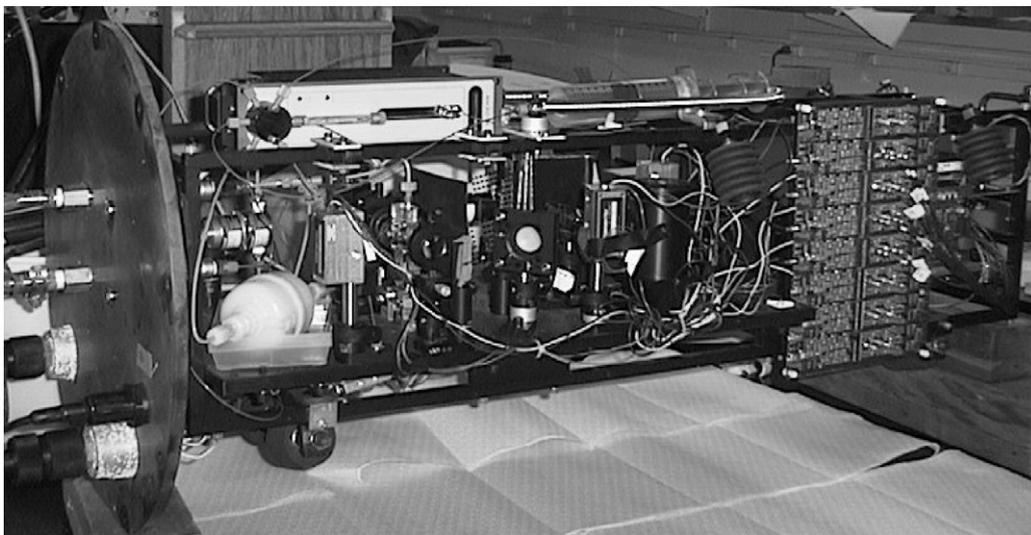
Fig. 3. Optics, fluidics, and electronics are mounted in a frame that rests on rubber wheels inside a 16 in diameter aluminum tube (removed here). At the top of the instrument, the syringe pump and bead reservoir are visible; on the left end is the bulkhead with sampling, data, and power connections; and at the right end are the signal conditioning electronics and computer. The optical components are in the center.

connecting to the shore-based computer via PCAnywhere sometimes interfered with data transfer from the instrument, we use a Web camera to observe the shore-based computer monitor remotely for routine checks when no intervention is planned.

2.1.4. Data analysis

For each particle, eight channels of signal data were stored (four parameters at two gain settings each), with a millisecond-resolution time stamp for each 200-event data transfer. The data were analyzed using software written in MATLAB (The Mathworks, Inc.). First, we calculated the volume of seawater analyzed as a function of time, taking into account periods when no data were being acquired (re-filling the sampling syringe and transferring data to shore) and merging the high- and low-gain data for each parameter. Next we obtained the number and properties of the standard beads in the samples in which they occurred. The data from the rest of the samples were then classified into one of several phyto-plankton populations. Phycoerythrin (PE)-positive cells (*Synechococcus* or cryptophytes) and PE-negative cells (encompassing all other phytoplankton) were classified on the basis of orange fluorescence. Within these groups, a customized clustering algorithm (utilizing side scattering and chlorophyll fluorescence data for each cell) was used to distinguish *Synechococcus* from crypto-phytes, and up to three groups of "eukaryotic phytoplankton". The distinction between large and small eukaryotic phytoplankton groups was not always obvious, so the use of the terms "picoeukaryotes" and "nanoeukaryotes" is only approximately correct for the data presented here.

2.2. Simple ducted flow with intersecting laser beams

We were initially concerned that disturbances in flow (e.g., from partial clogging or bubbles) would be a recurrent problem during unattended operation, so we explored the use of a simple ducted flow of seawater through the flow cell as an alternative to that of hydrodynamic focusing of the sample stream in a particle-free sheath stream. In this configuration, the Micro Pump pulled raw seawater through the flow cell at $5\,ml\,min^{-1}$, and

two tightly focused diode laser beams (Lasiris, 50 mW, 780 and 830 nm, respectively) were focused on the center of the flow cell (along with the third beam from the 532-nm laser, which was less tightly focused) to define the sensing region (Fig. 4). Only when light scattering signals from all three lasers occurred simultaneously (which meant that the particle in question had passed through the central, uniform, part of the green laser beam), were the signals from a given particle acquired.

2.3. Data quality

Flow cytometric data can be influenced by many factors other than the frequency and characteristics of the sample particles, including electronic noise, optical misalignment, and biased sampling. The capability to monitor the instrument during operation is therefore critical; the capability to make adjustments during operation is also desirable. FlowCytobot's operating mode includes periodic analyses of standard fluorescent plastic beads that serve to monitor optical alignment and stream flow in the flow cell. A suspension of beads (1 μm, red-fluorescing; Molecular Probes) in

a 120-ml reservoir (a spring-loaded plastic syringe) is sampled several times in succession at pre-programmed intervals (typically every 20 h), and analyzed analogously to the seawater samples. Because the beads eventually settle in the storage reservoir, we mixed the reservoir by attaching a magnet to the syringe pump arm and placing a magnetic stirring bar in the syringe; the stirring bar was dragged back and forth through the bead suspension with every syringe move.

Analysis of beads from an internal reservoir will not reveal problems with the seawater sampling system. This would require mixing beads with the seawater outside the instrument, which is beyond the capabilities of the present instrument. To prevent (or ameliorate) clogging of the seawater sample tube (or its 80-μm Nitex screen), the sampling program incorporates backflushing of the seawater sample tubing, as well as soaking it in detergent during the period when beads are being sampled.

To evaluate the performance of the instrument in actual use, we carried out a parallel sampling for analysis by conventional laboratory flow cytometry, on September 27, 2001 (when FlowCytobot
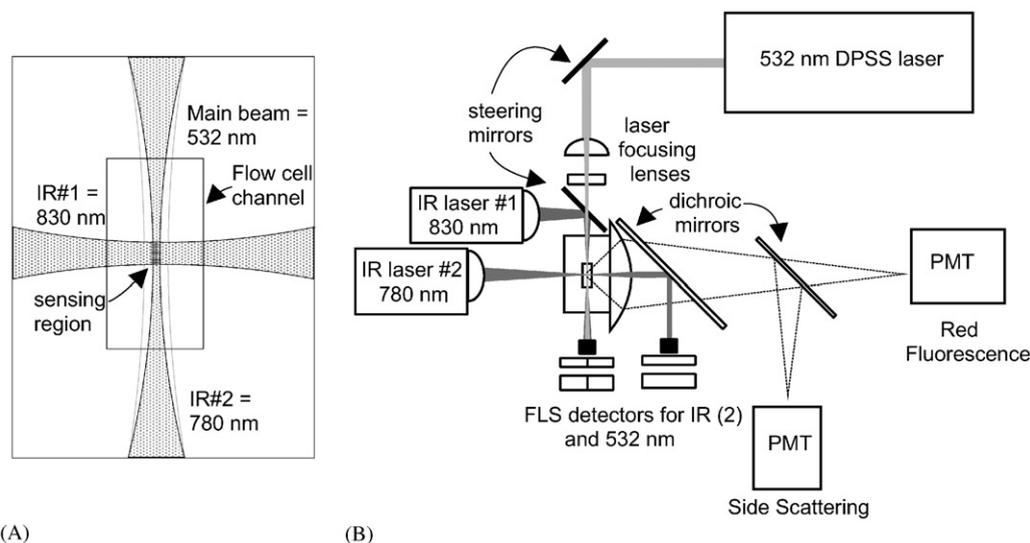
Fig. 4. Schema of flow cytometer layout during tests of an optically defined sensing region. (A) Cross-sectional view of the flow cell, where the intersection of two IR lasers defines a sensing region in the center of a third, 532 nm, laser beam. All three beams are in the same plane, with particles flowing upward through the flow cell channel. Data are acquired only from particles passing through all three beams simultaneously, ensuring that signal collection is triggered only when particles are in the central, uniform part of the green beam. (B) Layout of the optical and detection systems. For simplicity, not all lenses, dichroic mirrors and detectors are shown.

had been in operation at LEO-15 for 2 months). A sample obtained from 5-m depth at the LEO-15 site using a Niskin bottle was fixed with 0.1% glutaraldehyde and stored in liquid nitrogen, and was later analyzed at Woods Hole Oceanographic Institution (WHOI) with a modified Coulter EPICS flow cytometer (Green et al., 2003).

2.4. Size calibration

To enable us to estimate the size of phytoplankton cells, we calibrated FlowCytobot's light scattering measurements against measurements of cell volume as determined with a Coulter Multisizer, for 11 monospecific laboratory cultures of phytoplankton, ranging in diameter from ∼1 to 10 μm (as in Shalapyonok et al. 2001).

2.5. Deployment at LEO-15

The Longterm Ecosystem Observatory at 15 m (LEO-15) consists of two unmanned seafloor observatories 1.5 km apart, approximately 9 km off the central coast of New Jersey, and is designed to collect long-term oceanographic data with high temporal resolution (Glenn et al., 2000a). In situ instruments are deployed at the LEO site and connected to a fiber optic data/power link that transfers data, in real time, back to the shore station.

For deployment, FlowCytobot was mounted in an aluminum frame, which was clamped by divers into a platform anchored (by four pipes driven into the sediment) a few meters from node "B" (Fig. 5). Adjacent to the frame, a subsurface float with separate anchor supported a sample collection tube ($\frac{1}{2}$ in diameter Tygon) that was held at the desired depth (5 m at present) by attaching it to the subsurface float line. Electrical connection to the node is by separate power supply and communications cables with wet mate-able connectors and Kellums grips. We used the 120 V DC power available at the Guest Auxiliary Connector and the RS232 communications available at the Guest Main Connector. The raw data from FlowCytobot was transferred to shore after every
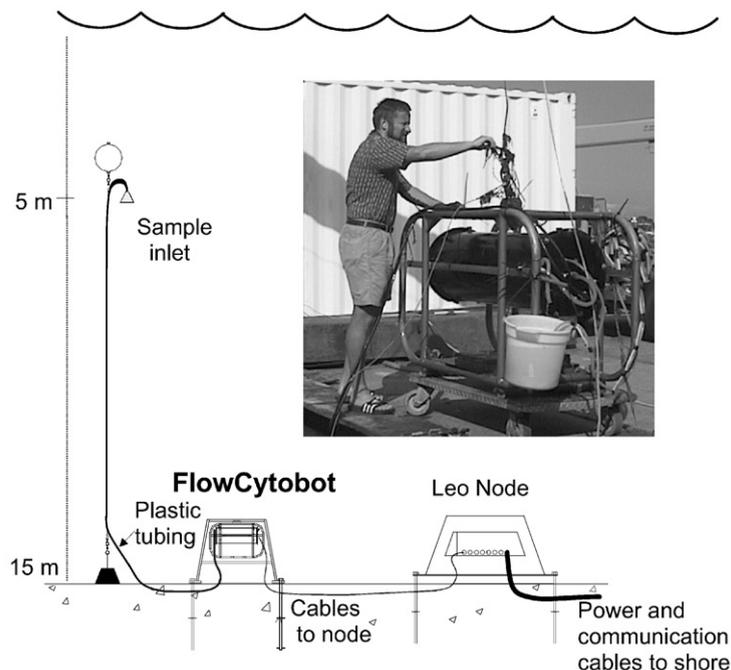
Fig. 5. Configuration of FlowCytobot at the LEO-15 mooring site off New Jersey. Inset: FlowCytobot in its frame, after testing off the WHOI dock.

200 events, at 9600 baud. Typical data acquisition rates were $2\,\mathrm{Mb}\,\mathrm{h}^{-1}$, representing $\sim 10^5$ cells analyzed in an hour. The data was stored on a dedicated computer, and periodically transferred over the Internet to the laboratory at WHOI for processing.

For tests off the WHOI dock or in the laboratory, power was supplied to FlowCytobot and communications were carried out via a 'LEO node simulator' constructed by C. van Alt at WHOI.

3. Results and discussion

3.1. Exploration of a simple ducted flow system

As an alternative to fluid focusing and the use of particle-free sheath fluid to force all sample particles through the center of the laser beam, we investigated an approach using a simple ducted flow of raw seawater and an optically defined sensing region (see Fig. 4). Our results indicated that such an approach is feasible but requires relatively complex data analysis involving assumptions about particle properties. Specifically, the Gaussian intensity profiles of the laser beams used to define the sensing region cause the sampling volume, and the distribution of particle sizes detected, to be a function of the light scattering properties of the particles. For example, while a small particle (i.e., with small light scattering) must pass through the central, most intense part of the IR beam to produce a signal above threshold, a larger particle may do so even if it passes through the outer edge of the beam. To obtain accurate cell concentrations, then, a scattering-dependent correction must be applied to the data. We empirically derived a correction algorithm by analyzing known mixtures of standard particles, and found that it was successful for correcting mixtures of different-sized phytoplankton (Fig. 6).

In addition, however, we found that a whole-seawater sample stream caused problems with the raw data when particles were very abundant. Cell signals often included light scattering from non-target particles present outside of the analysis region (but still in the main laser beam). These
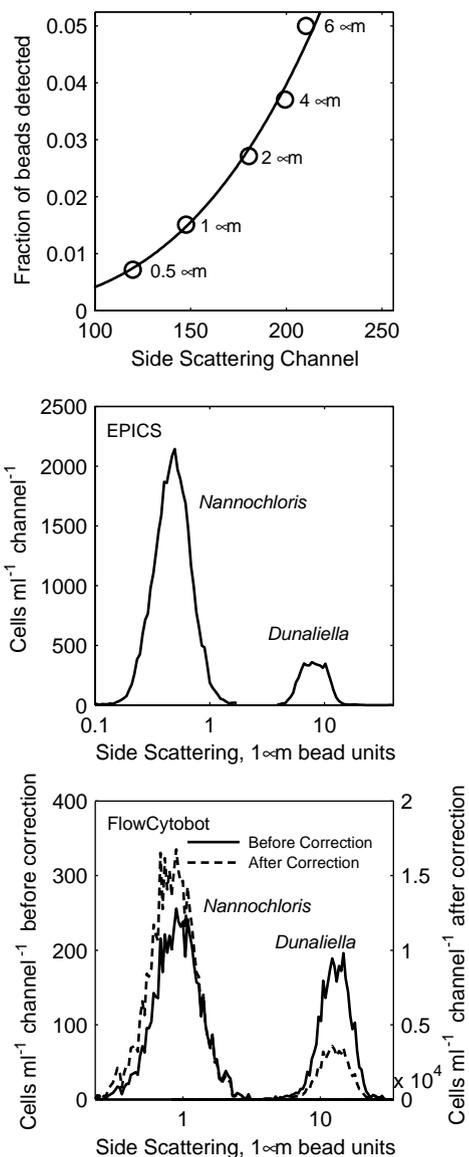
Fig. 6. With a simple ducted flow and optically defined sampling region, FlowCytobot's detection efficiency was size dependent (top panel). A correction algorithm was obtained by analyzing known concentrations of beads of different sizes. Cultures of phytoplankton of different sizes (*Dunaliella*, 8 μm; *Nannochloris*, 2.5 μm) were analyzed with the conventional flow cytometer (EPICS, middle panel), and with FlowCytobot using an optically defined sampling region (bottom panel); the large cells were detected with higher frequency than the small cells. After applying the bead-derived correction, cell concentrations from FlowCytobot (4600 and 34,000 cell ml^{-1} for *Dunaliella* and *Nannochloris*) were similar to those from the conventional flow cytometer (5800 and 39,000 cell ml^{-1}).

additions to the signals were usually small (presumably from bacteria or detritus, which are very numerous in coastal waters) but they caused the light scattering of small cells such as *Synechococcus* to be overestimated, and effectively limited the lower size of particles that could be analyzed. This problem could be reduced in laboratory tests by diluting the seawater sample with filtered seawater (data not shown), but this is not a practical solution for in situ sampling.

Because of this problem with the raw seawater approach (and because of its complexity in general), we returned to the "conventional" flow cytometric approach of injecting sample seawater into a filtered sheath stream.

3.2. Comparison of FlowCytobot and a laboratory flow cytometer

FlowCytobot is constructed in large part from conventional flow cytometer components, so it is not surprising that the performance of the two kinds of instruments is similar, as shown by parallel analyses of standard fluorescent beads and natural seawater samples. In laboratory tests, counting standard microspheres at concentrations up to 5×10^5 particles ml^{-1}, the two instruments gave similar results (Epics Count = 1.08*FlowCytobot Count, $r^2 = 0.99$, $n = 7$). FlowCytobot's analysis rate at the highest concentration tested (at a water sampling rate of 0.05 ml min^{-1}) corresponds to ~ 150 signals s^{-1}. To test effects on FlowCytobot of extended operation in the field, we compared its results with those of a water sample from approximately the same location and time, but analyzed by laboratory flow cytometry. Cell concentrations of populations defined by clustering on the basis of light scattering and fluorescence characteristics were similar for the two instruments (Fig. 7): EPICS and FlowCytobot gave results of 6500 and 6200, 540 and 300, and 11,200 and 8300 cell ml^{-1} for *Synechococcus*, cryptophytes, and "other eukaryotic phytoplankton", respectively. We cannot explain why all three populations were less numerous according to FlowCytobot, but we note that in the test shown here the two instruments were not analyzing exactly the same water sample; the EPICS results

are from a single preserved aliquot from a Niskin bottle sample, while the FlowCytobot results are from three 0.25-ml samples analyzed in situ over the course of an hour.

The cell-specific optical measurements are not directly comparable between the two instruments because of design differences. FlowCytobot's 532 nm excitation light is more efficiently absorbed by the antennae pigments of *Synechococcus* (at least in coastal strains with low-phycourobilin phycoerythrin) than that from the 488-nm laser in the EPICS. In contrast, accessory pigments of most eukaryotes absorb 532-nm light less efficiently than 488-nm light. This causes the chlorophyll fluorescence of *Synechococcus* as measured by FlowCytobot to be high relative to that of the eukaryotes (and suggests that *Synechococcus* cells are easily detected by FlowCytobot). Conversely, while FlowCytobot appears able to easily measure the small eukaryotes in coastal waters, it is not well suited for very small cells that lack phycoerythrin or carotenoid accessory pigments, such as open-ocean *Prochlorococcus*, which have very low absorption at 532 nm. Measuring such cells with FlowCytobot probably will require a blue solid-state laser with higher output than is presently available.

A less obvious difference in the flow cytometric signatures from the two instruments, that of the relative positions of the cells and beads in terms of light scattering, is presumably caused by differing light scattering collection angles (FlowCytobot's side light scattering detector integrates over a larger angular distribution than that of the EPICS) in combination with the specific volume scattering functions of cells and plastic beads. Calibration of measurements of light scattering with Coulter Multisizer measurements of cell volume suggests that FlowCytobot light scattering signals can be used to estimate cell size with confidence (Fig. 8). A power law function explained 99% of the variance between cell volume and side angle light scattering.

3.3. LEO-15 deployment

FlowCytobot was deployed at LEO-15 from late July to early October 2001. Beads from an internal
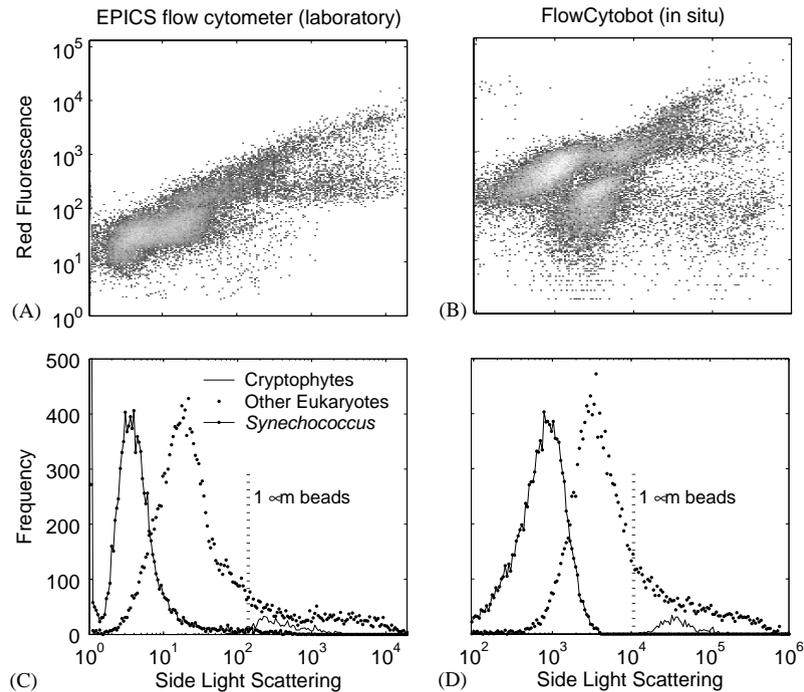
Fig. 7. Analyses of phytoplankton at LEO-15 measured by a Coulter EPICS flow cytometer (A, C) and by FlowCytobot (B, D). A discrete sample collected from the depth of FlowCytobot's sample intake at 12:00 on September 27, 2001, was analyzed with a modified EPICS flow cytometer (Green et al., 2003). The results are compared to those from FlowCytobot during the 1 h time period encompassing the Niskin sampling. The data are plotted in log units to show cells ranging in size from 1 μm (*Synechococcus*) to > 10 μm (cryptophytes and other eukaryotes). A and B are 2-parameter plots of all the particles with chlorophyll fluorescence, with lighter shading indicating higher concentrations of cells. Populations of cryptophytes, *Synechococcus*, and eukaryotic phytoplankton were discriminated as described in the text and their light scattering distributions presented separately in C and D. As expected, the appearance of the flow cytometric signatures is not identical (see text for details). The legend in C also applies to D.
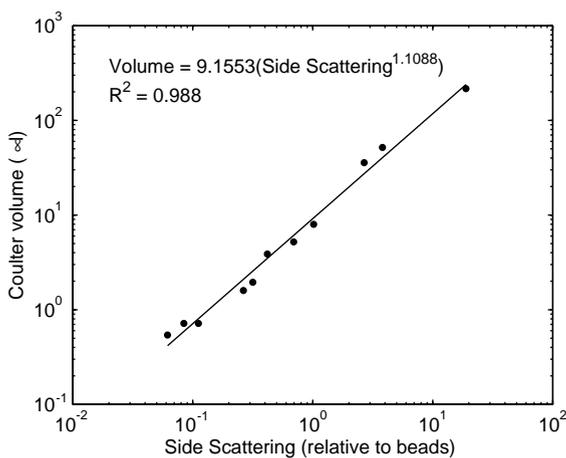
Fig. 8. Relationship between phytoplankton cell volume as measured with a Coulter Multisizer and side light scattering as measured by FlowCytobot. A power law function explained 99% of the variance between cell volume and side angle light scattering.

reservoir were analyzed approximately daily to monitor instrument performance (Fig. 9). A gradual decline in both concentration and mean bead optical properties was observed during the first month of the deployment, followed by a precipitous decline during the week of September 13; on September 17 we re-aimed the laser beam by remote control, which restored the optical signals nearly to their original values. Beads sinking or adhering to the walls of the reservoir may be responsible for the decline in bead concentration, but we cannot be sure. Likewise, we cannot be sure what caused the decline in sensitivity; it could have been caused by a shift in flow of the sample core stream, although the fact that the bead properties remained stable for many days after adjustment of the laser beam suggests that flow was not unstable and rather that the beam itself had shifted.
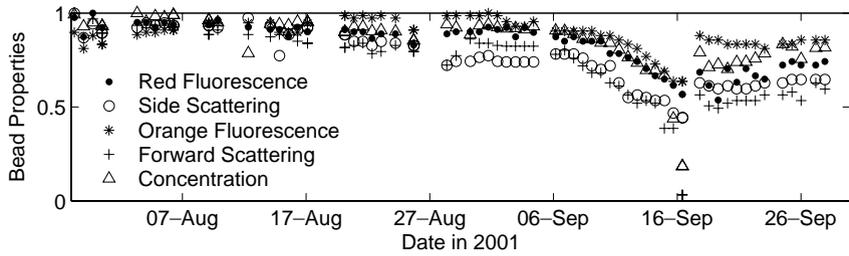
Fig. 9. Concentration and mean optical properties of internal standard beads analyzed during deployment at LEO-15.
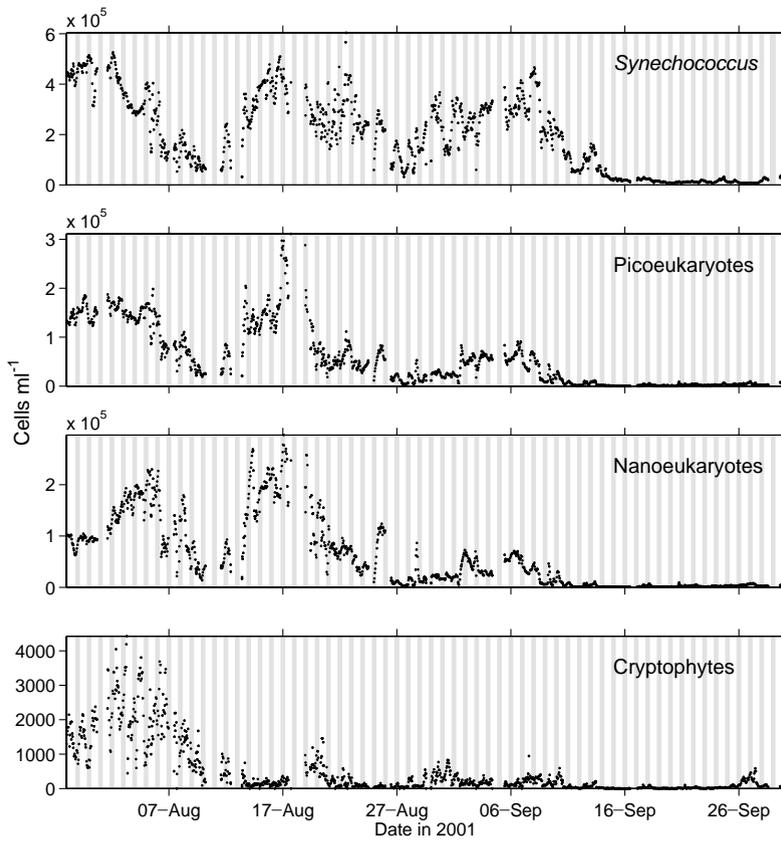
Fig. 10. Cell concentrations of different phytoplankton groups at LEO-15 as a function of time. Each datum represents an hourly mean value. Gray regions indicate night. Note that the distinction between large and small eukaryotic phytoplankton groups was not always obvious, and that the low numbers of cryptophytes present after the first week of the deployment often made measurements of this population unreliable.

Laboratory tank tests indicate that large changes in water temperature ($\sim 10°C$) can affect laser alignment, although on several occasions such changes in temperature were observed with no obvious effects on performance (data not shown).

The limiting factor in FlowCytobot's moored operation was wear and eventual leaking of the piston seal in the syringe used to move sample water. We believe this began after 2 months of continuous operation, suggesting that replacement
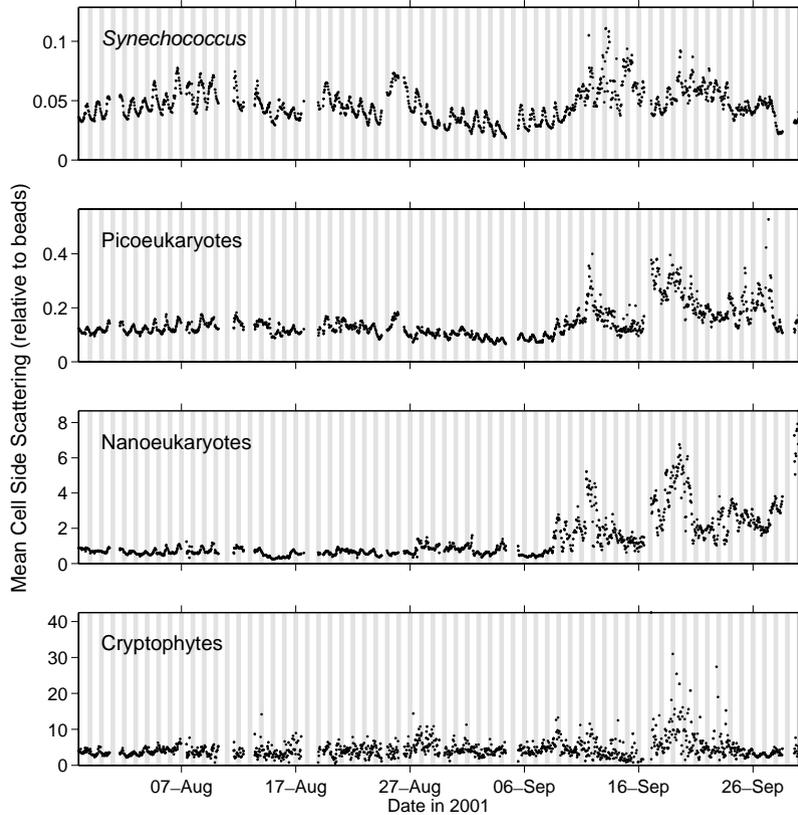
Fig. 11. Mean side light scattering (relative to 1 μm beads) of different phytoplankton groups as a function of time. Each datum represents an hourly mean value. Gray regions indicate night. Note that the distinction between large and small eukaryotic phytoplankton groups was not always obvious, and that the low numbers of cryptophytes present after the first week of the deployment often made measurements of this population unreliable.

of the syringe at intervals on this order will probably be necessary during sustained operation.

A second anticipated problem, that of sample contamination by cell growth in the Tygon tubing bringing water down to the instrument, was apparently not serious, based on our comparison with an independent water sample analysis. A third potential problem, fouling inside the instrument (flow cell, PEEK tubing, and filter cartridge), was apparently prevented effectively by the addition of sodium azide to the recirculating sheath fluid (final concentration ∼0.02%) and/or detergent treatments and backflushing of the sample tubing (see Fig. 1).

The optical signals for phytoplankton cells were normalized to the nearest bead sample, since we

believe these declines were caused by shifts in laser illumination or flow stream position, which would affect cells as well as beads. (We have not applied an adjustment to the cell concentration data; the observed changes in cell concentrations were far larger than those in bead concentrations so this would be a relatively small adjustment). Except during the event around September 17, the decline in bead concentration was probably not caused directly by declining optical sensitivity; the red fluorescence of the beads is several-fold higher than the detection threshold.

Large changes in cell concentration (∼2 orders of magnitude) were noted for all phytoplankton groups (Fig. 10), which could be due to physical mixing and advection of different water masses at
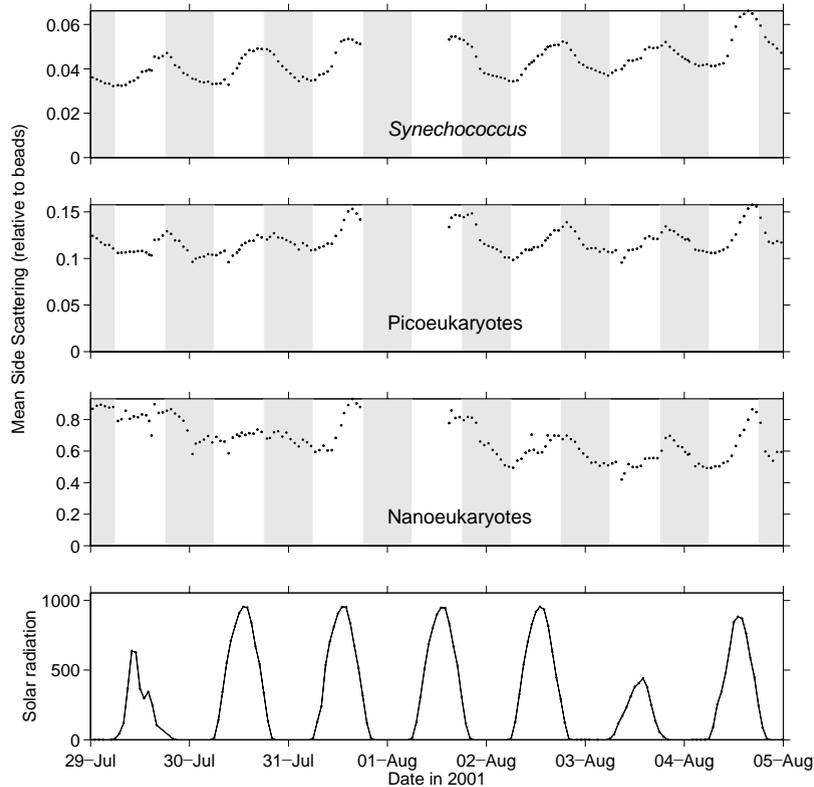
Fig. 12. Mean side light scattering (relative to 1 μm beads) of different phytoplankton groups at LEO-15 during the week of July 29 to August 5, 2001, and solar radiation (W m^{-2}, bottom panel) measured at a meteorological tower on shore. Each datum represents an hourly mean value. Gray regions indicate night. Communications problems between FlowCytobot and the shore station caused data to be lost around 1 August.

the sampling site. Changes in mean cell optical properties of each group were much smaller than for cell concentrations, on the order of 2-fold (Fig. 11), as expected for well-defined populations. In addition, closer examination reveals distinct diel patterns, especially in light scattering (Fig. 12). These patterns presumably reflect cell growth and division, as discussed elsewhere (Olson et al., 1990b; DuRand and Olson, 1996; Shalapyonok et al., 1998; Jacquet et al., 2001); in both *Synechococcus* and eukaryotic phytoplankton, mean cell light scattering increased during the day and decreased at night. The decrease sometimes began earlier in the case of *Synechococcus*, consistent with the finding that cell division in *Synechococcus* occurs in daylight hours (Waterbury et al., 1986), earlier than at least some other

kinds of phytoplankton (Vaulot and Marie, 1999; Jacquet et al., 2001; Binder and DuRand, 2002).

The large declines in cell concentrations that occurred in September were accompanied by water column mixing that may have reduced cell growth rates through light limitation (Sosik et al., 2003). The increases in cell light scattering during the same time period could be related to such lowered growth rates, but could also reflect changing species composition.

4. Conclusion

Although there are several aspects of FlowCytobot that can be improved (e.g., we hope to reduce its size, increase its sampling rate, and

improve its reliability), the deployment at LEO-15 demonstrates that in situ flow cytometric measurements of phytoplankton are practical, and that this approach can provide quantitative information over an unprecedented range of time scales. The observed diel patterns in cell size can reveal growth rates of the phytoplankton even though the patterns in cell concentration are dominated by non-biological mechanisms such as water mass exchange (Sosik, et al., submitted), and should help us to understand the dramatic changes in cell populations observed on longer time scales. Longer deployments, in concert with more comprehensive environmental and hydrographic measurements, are now needed.

Acknowledgements

References

André, J.-M., Navarette, C., Blanchot, J., Radenac, M.-H., 1999. Picophytoplankton dynamics in the equatorial pacific: growth and grazing rates from cytometric counts. Journal of Geophysical Research 104, 3369–3380.

Binder, B.J., DuRand, M.D., 2002. Diel cycles in surface waters of the equatorial Pacific. Deep-Sea Research II 49, 2601–2617.

Chisholm, S.W., 1992. Phytoplankton size. In: Falkowski, P.G., Woodhead, A.D. (Eds.), Primary Productivity and Biogeochemical Cycles in the Sea. Plenum, New York, pp. 213–237.

Cloern, J.E., 2001. Our evolving conceptual model of the coastal eutrophication problem. Marine Ecology Progress Series 210, 223–253.

Dubelaar, G.B.J., Gerritzen, P.L., Beeker, A.E.R., Jonker, R.R., Tangen, K., 1999. Design and first results of cytobuoy: a wireless flow cytometer for in situ analysis of marine and fresh waters. Cytometry 37, 247–254.

DuRand, M.D., Olson, R.J., 1996. Contributions of phytoplankton light scattering and cell concentration changes to diel variations in beam attenuation in the equatorial Pacific

from flow cytometric measurements of pico-, ultra- and nanoplankton. Deep-Sea Research (Part 2, Topical Studies in Oceanography) 43, 891–906.

DuRand, M.D., Olson, R.J., 1998. Diel patterns in optical properties of the chlorophyte Nannochloris sp.: relating individual-cell to bulk measurements. Limnology and Oceanography 43, 1107–1118.

DuRand, M.D., Olson, R.J., Chisholm, S.W., 2001. Phytoplankton population dynamics at the Bermuda Atlantic time-series station in the Sargasso Sea. Deep-Sea Research (Part 2, Topical Studies in Oceanography) 48, 1983–2003.

Glenn, S.M., Boicourt, W., Parker, B., Dickey, T.D., 2000a. Operational observation networks for ports, a large estuary and an open shelf. Oceanography 13, 12–23.

Glenn, S.M., Dickey, T.D., Parker, B., Boicourt, W., 2000b. Long-term real-time coastal ocean observation networks. Oceanography 13, 24–34.

Green, R.E., Sosik, H.M., Olson, R.J., DuRand, M.D., 2003. Flow cytometric determination of size and complex refractive index for marine particles: comparison with bulk measurements. Applied Optics 42, 526–541.

Jacquet, S., Partensky, F., Lennon, J., Vaulot, D., 2001. Diel patterns of growth and division in marine picoplankton in culture. Journal of Phycology 37, 357–369.

Kerkhof, L.M., Voytek, D.F., Mille, R.S., Schofield, O., 1999. Variability in bacterial community structure during upwelling in the coastal ocean. Hydrobiologia 401, 139–148.

Li, W.K.W., Dickie, P.M., 2001. Monitoring phytoplankton, bacterioplankton, and virioplankton in a coastal inlet (Bedford Basin) by flow cytometry. Cytometry 44, 236–246.

Olson, R.J., Chisholm, S.W., Zettler, E.R., Altabet, M.A., Dusenberry, J.A., 1990a. Spatial and temporal distributions of prochlorophyte picoplankton in the North Atlantic Ocean. Deep-Sea Research 37, 1033–1051.

Olson, R.J., Chisholm, S.W., Zettler, E.R., Armbrust, E.V., 1990b. Pigments, size, and distribution of *Synechoccus* in the North Atlantic and Pacific oceans. Limnology and Oceanography 35 (1), 45–58.

Olson, R.J., Zettler, E.R., Chisholm, S.W., 1991. Advances in oceanography through flow cytometry. In: Demers, S. (Ed.), Particle Analysis in Oceanography. Verlag, Weinheim, pp. 351–399.

Olson, R.J., Zettler, E.R., DuRand, M.D., 1993. Phytoplankton analysis using flow cytometry. In: Kemp, P.F., Sherr, B.F., Sherr, E.B., Cole, J.J. (Eds.), Aquatic Microbial Ecology. Lewis Publishers, Boca Raton, pp. 175–186.

Pearce, J.B., Berman, Jr., C.R., Rosen, M. R., 1982. Annual NEMP Report on the Health of the Northeast Coastal Waters, NMFS-F/NEC-35, Northeast Fisheries Center, Woods Hole, MA.

Reckermann, M., Colijn, F.(Eds.), 2000. Aquatic Flow Cytometry: Achievements and Prospects. Scientia Marina 64(2), Barcelona.

Schofield, O., Bergmann, T., Bissett, W.P., Grassle, F., Haidvogel, D., Kohut, J., Moline, M., Glenn, S., 2002. The long-term ecosystem observatory: An integrated coastal

observatory. IEEE Journal of Oceanic Engineering 27, 146–154.

Shalapyonok, A., Olson, R.J., Shalapyonok, L.S., 2001. Arabian Sea phytoplankton during Southwest and Northeast Monsoons 1995: composition, size structure and biomass from individual cell properties measured by flow cytometry. Deep-Sea Research (Part 2, Topical Studies in Oceanography) 48, 1231–1262.

Shalapyonok, A.A., Olson, R.J., Shalapyonok, L.S., 1998. Ultradian growth in prochlorococcus spp. Applied and Environmental Microbiology 64, 1066–1069.

Sosik, H.M., Olson, R.J., Neubert, M.G., Shalapyonok, A.A., Solow, A.R., 2003. Growth rates of coastal phytoplankton populations from time-series measurements with a submersible flow cytometer.Limnology, Oceanography, submitted for publication.

Vaulot, D., Marie, D., 1999. Diel variability of photosynthetic picoplankton in the equatorial pacific. Journal of Geophysical Research 104, 3297–3310.

Vaulot, D., Marie, D., Olson, R.J., Chisholm, S.W., 1995. Growth of *prochlorococcus,* a photosynthetic prokaryote, in the equatorial pacific ocean. Science 268, 1480–1482.

Waterbury, J.B., Watson, S.W., Valois, F.W., Franks, D.G., 1986. Biological and ecological characterization of the marine unicellular cyanobacterium *Synechococcus.* In: Platt, T., Li, W.K.W. (Eds.), Photosynthetic Picoplankton, Vol. 214. Candian Bulletin of Fisheries and Aquatic Sciences, Ottawa, pp. 71–120.